

高密度電漿之後處理對奈米碳管場發射特性之影響

研究生：王文彬

指導教授：鄭晃忠 博士

國立交通大學電機資訊學院 電子與光電學程（研究所）碩士班

摘 要

奈米碳管(Carbon Nanotubes, CNTs)，因為具有極好的高寬比、小的曲率半徑、良好的化學穩定性、以及很高的機械強度，所以已經被大量應用於場發射元件之製程上。奈米碳管陣列的場發射電流強烈依賴功函數及奈米碳管表面的幾何形狀，優異的場發射特性具有較低的場發射電場以及較高的場發射電流密度。

在場發射材料的合成部分，利用熱化學氣相沉積(Thermal Chemical Vapor Deposition)系統探討以鐵-鎳合金為催化金屬層，藉由控制奈米碳管成長的參數來合成不同形態的奈米碳管。此外由場發射的測試中可以發現，奈米碳管具有非常優異的場發射特性，然而密度較高($\sim 10^{12}/\text{cm}^2$)的奈米碳管因為電場之遮蔽效應(screening effect)，使得場發射特性並不

因其具有較高密度之場發射源而變好。此論文為了進一步改善奈米碳管之場發射特性，提出了利用高密度電漿(氫、氧)蝕刻之後處理來改變奈米碳管之密度以降低電場之遮蔽效應。

實驗結果證實在適當的條件之下，奈米碳管之場發射起始電場可以大幅降低(由 $3.1 \text{ V}/\mu\text{m}$ 下降至 $2.2 \text{ V}/\mu\text{m}$)，而場發射電流亦可大幅增加(由 $2.35 \text{ mA}/\text{cm}^2$ 上升至 $48 \text{ mA}/\text{cm}^2$ 當操作電場在 $5 \text{ V}/\mu\text{m}$)。同時在 SEM 材料分析儀器分析下，證實了奈米碳管的分佈與表面型態的確因高密度電漿(氫、氧)之後處理而改變。主要的原因是氫電漿以物理反應方式能夠有效地改變在奈米碳管上缺陷部分(非晶質碳)及揮發性污染物。氧電漿以化學反應方式改變奈米碳管表面結構如同去除非晶矽碳管，形成頂端的開口和減少奈米碳管層數，經由化學反應產生 CO 、 CO_2 等揮發性氣體而改善了奈米碳管的密度。

為了符合場發射顯示器低電壓操作的目的，實驗以半導體製程技術製作閘極來形成奈米碳管三極元件，並利用擇性成長奈米碳管的技術，以及控制奈米碳管成長密度的方式，將閘極操作電壓降低到 30 伏特。

Effects of High Density Plasma Post Treatments on the Characteristics of Carbon Nanotube Field Emission Displays

Student : Wen-Pin Wang

Advisors : Prof. Huang-Chung Cheng

Degree Program of Electrical Engineering Computer Science
National Chiao Tung University

ABSTRACT

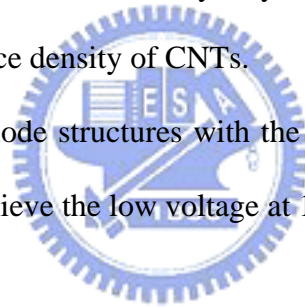
Carbon nanotubes (CNTs) have been applied for the process of the field emission devices, because of their high aspect ratio, small radius curvature, high chemical stability, and high mechanical strength. Field emission current of CNT arrays depends strongly on the work function and geometry of the surface of CNT arrays. Excellent field emission properties of CNTs have been demonstrated lower turn-on electric field and higher field emission current density.

For the synthesis of field emission materials, carbon nanotubes (CNTs) with various morphologies have been synthesized using thermal chemical vapor deposition (Thermal CVD) with Fe-Ni alloy catalysts via controlling the parameters of CNTs growth. The CNT emission arrays showed excellent field emission properties, however, the field emission properties of the high density CNTs ($\sim 10^{12}/\text{cm}^2$) degraded for the screening effect of the electric field. To improve the field emission properties of the CNTs, a novel post treatment process with plasma etching to reduce the screening effect of the electric field have been proposed.

The results depicted that the field emission properties can be upgraded with proper high density plasma treatment conditions. A plasma post treatment was introduced to

reduce the density of CNTs. Scanning electron microscopy (SEM) micrographs showed reduced densities of the CNTs, and the measurement of electrical characteristics revealed the improved field emission properties under suitable plasma conditions. The turn-on electrical field decreased from 3.1 V/ μm to 2.2 V/ μm , and the emission current density increased from 2.35 mA/cm² to 48 mA/cm² at the applied field of 5 V/ μm . SEM have verified that the distribution and surface morphology of CNTs have been changed by HDPPT (argon , oxygen). The plasma exposure to argon (Ar) gas was performed in situ in order to modify all structural defects (non-crystalline carbon) and contamination of CNTs . Oxygen plasma removed the structure of carbon nanotubes on the surface, such as removing amorphous carbon, exhibiting the open-end on the tip and reducing the walls of carbon nanotube by way of chemical reaction, produce CO , CO₂ volatility gas and influence density of CNTs.

Finally, the CNT triode structures with the proposed plasma post treatments have been demonstrated to achieve the low voltage at 18V.



誌 謝

三年的碩士生涯中，首先要感謝國立交通大學所有教導過我的老師，尤其是我的指導教授—鄭晃忠老師，謝謝他在論文研究和為人處世方面的指導與鼓勵，才能使我順利地完成碩士學位。

其次，要感謝交通大學半導體中心（SRC）和國家毫微米實驗室（NDL）提供完善的實驗設備，尤其是要感謝半導體研究中心的技術人員—何惟梅小姐、徐秀鑾小姐、黃月美小姐、陳聯珠小姐、林素珠小姐他們在實驗設備及維護上給予最大的支持與協助，使我的研究得以順利完成。

同時感謝實驗室的夥伴，全平學長、志良學長、春乾學弟、高照學弟、瑞霖學弟、宗穎學弟、耀仁學弟、鈞凱學弟、翰忠學弟、材料所慶榮同學、機械所華強同學、奈米所天佑學弟、以及其他的人等等，有你們在實驗與生活上的鼓勵和協助，漫長的求學生涯才顯得多采多姿。而諸位口試委員的建議與指正，在此也一併表達感謝之意。

最後，我要特別感謝我的母親黃清香女士、我的妻子陳明玲女士、台達電子視訊事業部副總經理潘國華先生、以及其他的人等等，這些年來對我全力的支持與照顧，讓我無後顧之憂，得以順利完成學業。除此之外，我亦要感謝我的家人給我的鼓勵與付出。謹以此論文獻給我最親愛的家人與朋友。

Contents

| | | |
|---|---|-----------|
| Abstract (in Chinese) | i | |
| Abstract (in English) | iii | |
| Acknowledgments (in Chinese) | v | |
| Contents | vi | |
| Table Lists | ix | |
| Figure Captions | x | |
| Symbols | xiv | |
| Chapter 1 | Introduction | 1 |
| 1.1 | History of Vacuum Microelectronics | 1 |
| 1.1.1 | Overview of Vacuum Microelectronics | 1 |
| 1.1.2 | Theory Background | 2 |
| 1.2 | Applications of Vacuum Microelectronics | 5 |
| 1.2.1 | Vacuum Microelectronic Devices for Electronic Circuits | 6 |
| 1.2.2 | Field Emission Display | 6 |
| 1.3 | Recent Developments of Field Emission Devices for Field Emission Displays | 8 |
| 1.3.1 | Cathode Structure and Materials for Field Emission Displays..... | 8 |
| 1.4 | Motivation | 11 |
| 1.5 | Thesis Organization | 12 |
| Chapter 2 | Overview | 13 |
| 2.1 | Introduction | 13 |
| 2.2 | Structures and Characteristics of Carbon Nanotubes | 13 |
| 2.3 | The methods of carbon nanotubes synthesis | 15 |
| 2.4 | The mechanism of CNTs growth | 16 |
| 2.4.1 | CNT Growth Mechanism | 17 |
| 2.4.2 | Influence of the metal-support interaction for tip growth mode and base growth (root growth) mode | 17 |

| | | |
|------------------|--|-----------|
| 2.4.3 | The defects of CNTs | 18 |
| Chapter 3 | Experimental Procedures | 19 |
| 3.1 | Synthesis and Properties of Carbon Nanotubes for Field Emission Diode Devices | 19 |
| 3.1.1 | Sample preparation | 19 |
| 3.1.2 | Buffer layer and metal catalyst deposition by Sputter & Electron beam evaporation (E-GUN) | 19 |
| 3.1.3 | CNTs growth by Thermal CVD | 20 |
| 3.1.4 | Controlled Density of CNTs by HDP – RIE Post-Treatment | 20 |
| 3.2 | Fabrication of Carbon Nantubes for Field Emission Triode Device | 20 |
| 3.2.1 | Sample preparation | 20 |
| 3.2.2 | Buffer Layer and Metal Catalyst Deposition by Sputter & Electron beam evaporation (E-GUN) | 21 |
| 3.2.3 | CNTs Growth by Thermal CVD | 21 |
| 3.2.4 | Controlled Density of CNTs by HDP-RIE Post-Treatment | 22 |
| 3.3. | Measurement System | 22 |
| 3.3.1 | Field emission measurement | 22 |
| 3.3.2 | Scanning Electron Microscopy (SEM) was Employed for the Analysis of the Morphology and Density CNTs | 23 |
| 3.3.3 | The CNTs were Characterized by Raman Spectroscopy | 23 |
| 3.3.4 | High-Resolution Transmission Electron Microscopy (TEM) was Adopted for the Microstructure Analysis of CNTs | 23 |
| 3.3.5 | An Energy Dispersive X-Ray (EDX) Analyzer was Used to Investigate the Composition of the Fe-Ni Surface after Plasma Post Treatment | 23 |
| Chapter 4 | Results & Discussion | 24 |
| 4.1 | Synthesis and Characteristics of Carbon Nanotubes by Thermal CVD..... | 25 |
| 4.1.1 | Effects of Catalyst Layer Thickness | 25 |
| 4.1.2 | Effects of Pre-Treatment and Deposition Temperature | 26 |
| 4.1.3 | Effects of the C ₂ H ₄ for CNT Length | 28 |
| 4.2 | Effects of Field Emission on the Characteristics of Carbon Nanotubes Diodes High-Density-Plasma Post Treatment | 29 |

| | | |
|----------------------|--|-----------|
| 4.2.1 | Mechanism of HDPPT | 29 |
| 4.2.2 | Effects of High Density Plasma (HDP) Reaction ion etching (RIE) Post Treatment of Argon (Ar) on the characteristics of CNTs | 31 |
| 4.2.3 | Effects of High Density Plasma (HDP) Reaction ion etching (RIE) Post Treatment of Oxygen (O ₂) on the characteristics of CNTs | 33 |
| 4.2.4 | Effects of High Density Plasma (HDP) Reaction ion etching (RIE) Post Treatment of Argon (Ar) and Oxygen (O ₂) Mixture on the characteristics of CNTs | 36 |
| 4.3 | Fabrication and Characteristics of the Carbon Nantubes Field Emission Triodes with HDPPT | 37 |
| Chapter 5 | Summary and Conclusions | 39 |
| Figures | | 42 |
| Tables | | 88 |
| References | | 91 |
| Autobiography | | 98 |



Table Lists

Chapter 3

Table 3-1 : Conditions of different pretreatment times and catalyst layer thickness...55

Table 3-2 : Conditions of C₂H₄ flow rate for CNT growth lengths(700°C).....55

Table 3-3 : Conditions of Ar or/and O₂ mixture gas HDPPT for diode.....56

Table 3-4 : Conditions of Ar or/and O₂ mixture gas HDPPT for diode with bias power (fixed ICP power 300W).....56

Chapter 4

Table 4-1 : Comparison physical versus chemical plasma etching.....88

Table 4-2 : Shows effects of changing plasma etching parameters.....88

Table 4-3 : Summary Ar and O₂ HDPPT for different flow rates VS different ICP Powers on turn-on field, emission current density, and field enhancement factor.....89

Table 4-4 : Summary Ar and O₂ HDPPT for different BIAS Powers on turn-on field, emission current density, and field enhancement factor.....90

Figure Captions

Chapter 1

- Fig. 1.1 Energy diagrams of vacuum-metal boundary: (a) without external electric field, (b) with an external electric field, and (c) Tunneling phenomenon.....42
- Fig. 1.2 (a) Simulation of field penetration, (b) Distance between emitters versus geometrical enhancement factors.....43
- Fig. 1.3 (a) CRT (Cathode Ray Tube), (b) VFD (Vacuum Fluorescent Display), (c) PDP (Plasma Display Panel), and (d)(e) CNT FED (Carbon Nanotube Field Emission Display).....44
- Fig. 1.4 (a) Sony portable DVD player using a Candescant field emission display, (b) Motorola 15" field emission display, (c) Motorola 5.6" color FED, (d) Pixtech 5.6" color FED, (e) Futaba 7" color FED, and (f) 7" color CNT FED from Samsung.....45

Chapter 2

- Fig. 2.1 High-resolution transmission electron microscopy images of (a) single-walled nanotubes (SWNTs) and (b) multiwalled nanotubes (MWNTs). Every layer in the image (fringe) corresponds to the edges of each cylinder in the nanotube assembly.....46
- Fig. 2.2 Illustrations of the atomic structure of (a) an armchair and (b) a zig-zag nanotube, (c) The Stone-Wales transformation occurring in an armchair nanotube under axial tension.....46
- Fig. 2.3 Molecular models of single-walled nanotubes with different helicities: (a) zig-zag arrangement; (b) armchair configuration; (c) and (d) two different helicities.....46
- Fig. 2.4 (a) The chiral vector OA is defined on the honeycomb lattice of carbon atoms by unit vectors a_1 , a_2 and the chiral angle θ with respect to the zigzag axis, (b) Possible vectors specified by the pairs of integers (n,m) for general carbon tubules, including zigzag, armchair, and chiral tubules, (c) Schematic diagram showing how a hexagonal sheet of graphite is 'rolled' to form a carbon nanotube.....47

| | | |
|----------|---|----|
| Fig. 2.5 | (a) Schematic diagram of an arc evaporator, (b) Schematic of the laser ablation process, (c) Schematic of the thermal chemical vapor deposition, and (d) Schematic of the microwave plasma enhanced chemical vapor deposition (MPECVD)..... | 47 |
| Fig. 2.6 | (a) hydrocarbon dissociate & deposit carbon on surface, (b) carbon diffuses through solid metal, and (c) carbon precipitates as curved graphitic layers [78]..... | 48 |
| Fig. 2.7 | Influence of the metal-support interaction on the mode of filamentous for (a) base growth (root growth) mode, (b) tip growth mode, and (c) Combined tip growth and base growth..... | 48 |

Chapter 3

| | | |
|----------|---|----|
| Fig. 3.1 | Experimental procedures flow charts..... | 49 |
| Fig. 3.2 | (a)~(h) Fabrication procedure of the carbon nanotubes for diode structure field emission device..... | 50 |
| Fig. 3.3 | (a)~(c) High density plasma post treatment for diode device..... | 50 |
| Fig. 3.4 | (a)~(p) Fabrication procedure of the carbon nanotubes insulated gate structure field emission device (a)~(p)..... | 52 |
| Fig. 3.5 | (a)~(c) High density plasma post treatment for triode device (a)~(c)..... | 52 |
| Fig. 3.6 | Experimental procedure by Thermal CVD process..... | 53 |
| Fig. 3.6 | Schematic of emission measurement for (a) diode type and (b) triode type... | 54 |

Chapter 4

| | | |
|----------|---|----|
| Fig. 4.1 | Effects of pretreatment 15min for different catalyst layer thickness (a) 50Å, (b) 75Å, (c) 100Å, (d) 150Å, (e) plot of average nanoparticle size and CNT length as a function the Fe-Ni thickness, and (f) summary catalyst metal thickness versus nanoparticle size and CNT lengths..... | 58 |
| Fig. 4.2 | Effects of addition CH ₄ with pretreatment (a) without CH ₄ , (b) with CH ₄ (C ₂ H ₄ 20sccm, 500°C, 15minutes), (c) without CH ₄ , (d) with CH ₄ (C ₂ H ₄ 20sccm, 500°C, 15minutes)..... | 59 |
| Fig. 4.3 | Effects of CNTs growth (a) without N ₂ (b) with N ₂ and (c) TEM image for bamboo-like CNTs, and (d) bamboo-like CNTs mechanism..... | 61 |
| Fig. 4.4 | SEM images for different C ₂ H ₄ flow rate (a) 20sccm, (b) 50sccm, (c) 70sccm, | |

| | | |
|-----------|--|----|
| | (d) 138sccm, (e) effects of different growth temperature versus flow rate, and (f) summary experimental results for CNT lengths and different growth temperature..... | 63 |
| Fig. 4.5 | TEM image for growth mechanism on thermal CVD (a) base growth, (b)(c) with/without the catalyst on base growth, (d)(e) top growth, and (f) catalyst metal inside..... | 64 |
| Fig. 4.6 | (a) Physical etching mechanism, (b) chemical etching mechanism, and (c) combined physical and chemical etching mechanism..... | 65 |
| Fig. 4.7 | SEM images of CNTs post-treatment by Ar 10sccm 60sec for different ICP power of (a) as-grown, (b) 250W, (c) 300W, (d)400W, (e) 500W, (f) Raman spectra of CNTs, (g) field emission curve J-E, (h) F-N plot, and (i) summary experimental results..... | 67 |
| Fig. 4.8 | SEM images of CNTs post-treatment by Ar 20sccm 60sec for different ICP power of (a) as-grown, (b) 250W, (c) 300W, (d)400W, (e) 500W, (f) Raman spectra of CNTs, (g) field emission curve J-E, (h) F-N plot, and (i) summary experimental results..... | 68 |
| Fig. 4.9 | SEM images of CNTs post-treatment by Ar 30sccm 60sec for different ICP power of (a) as-grown, (b) 250W, (c)300W, (d)400W and (e)150W, (f) field emission curve J-E, (g) F-N plot, and (h) summary experimental results..... | 71 |
| Fig. 4.10 | SEM images of CNTs post-treatment by Ar 30sccm 60sec for different ICP power of (a) as-grown, (b) 250W, (c)300W, (d)400W and (e)150W, (f) field emission curve J-E, (g) F-N plot, and (h) summary experimental results..... | 73 |
| Fig. 4.11 | SEM images of CNTs post-treatment by Ar 20sccm ICP power 300W 60sec for different BIAS power of (a) 0W, (b) 50W, (c) 100W, (d)150W, (e) Raman spectra of CNTs, (f) field emission curve J-E, (g) F-N plot, and (h) summary experimental results..... | 75 |
| Fig. 4.12 | SEM images of CNTs post-treatment by O ₂ 5sccm 60sec for different ICP power of (a) as-grown, (b) 250W, (c) 300W, (d) 400W, (e)500W, (f) Raman spectra of CNTs, (g) field emission curve J-E, (h) F-N plot, and (i) summary experimental results..... | 77 |
| Fig. 4.13 | SEM images of CNTs post-treatment by O ₂ 10sccm 60sec for different ICP power of (a) as-grown, (b) 250W, (c) 300W, (d) 400W, (e)500W, (f) field emission curve J-E, (g) F-N plot, and (i) summary experimental results..... | 79 |
| Fig. 4.14 | SEM images of CNTs post-treatment by O ₂ 20sccm 60sec for different ICP | |

power of (a) as-grown, (b) 250W, (c) 300W, (d) 400W, (e)500W, (f) field emission curve J-E, (g) F-N plot, and (i) summary experimental results.....81

Fig. 4.15 SEM images of CNTs post-treatment by O₂ 10sccm ICP power 300W 60sec for different BIAS power of (a) 0W, (b) 50W, (c) 100W, (d) 150W, (e) Raman spectra of CNTs , (f)field emission curve J-E, (g) F-N plot, and (h) summary experimental results.....83

Fig. 4.16 SEM images of CNTs post-treatment by Ar 20sccm and O₂ 10sccm mixture gas with ICP power 300W 60sec for BIAS power (a) as grown, (b) without BIAS power, (c) with BIAS power, (d)field emission curve J-E, (e) F-N plot, and (f) summary experimental results.....85

Fig. 4.17 SEM images of CNTs post-treatment for PPT (a) as-grown (b) Ar 20sccm for ICP power 300W 60sec (c) Ar 20sccm for ICP power 300W 60sec with BIAS power 100W(d) O₂ 10sccm for ICP power 300W 60sec (h) field emission curve I-V, and (f) summary field emission results87



Symbols

W_0 : the energy difference between an electron at rest outside the metal and an electron at

rest inside the metal

W_f : the energy difference between the Fermi level and the bottom of the conduction band

ϕ : work function

J : the current density (A/cm^2)

E : the applied electric field (V/cm)

α : the emitting area

β : the local field enhancement factor

S : Slope_{FN} the slope of a Fowler-Nordheim (F-N) plot

r : the tip radius of emitter tip

d : the emitter-anode(gate) distance

β^* : geometric correction factor

E_{tip} : realistic electric field in the emitter tip

g_m : transconductance

